A LES Scheme for Mixing and Reacting Flow Inside a Combustor

Álvaro L. De Bortoli

UFRGS - Department of Pure and Applied Mathematics,
Bento Gonçalves 9500, P.O. Box 15080, Porto Alegre, Brazil
dbortoli@mat.ufrgs.br

Abstract. The present work develops a LES scheme for the solution of mixing and reacting flows inside a combustor. The model considers the overall, single step, irreversible reaction between two species; the reaction rate is governed by the Arrhenius law. Numerical tests, based on the finite difference explicit Runge-Kutta five-stage scheme, for third order time and fourth order space approximations, are carried out for Damköhler 300, Zel'dovich 10, Heat Release 10 and Schmidt and Prandtl both equal to 0.9 and the results contribute to understand the mixture-reaction behaviour for the reacting flow inside a combustor.

1 Introduction

Many applications of technical interest in combustion are based on non-premixed or diffusion flames. In a diffusion flame the reaction occurs at interface of the fuel and the oxidiser. Being the reactants supplied in separate streams, they are not complete mixed before burning; therefore, to model non-premixed flames it is necessary a good understanding of combustion processes and of turbulent mixing [8] where hypothesis are necessary and they need to be clearly defined, understood and consistent.

Combustion flows involve a large range of time and length scales; most of the kinetic energy is carried by the large scale structures, which depends on the geometry of the flow field. Inside the flame the gas expand rapidly and form low density regions which effectively process the mixing [2].

Combustion models may turn very complex: the complete mechanism of the methane combustion has been identified as having more than 300 elementary reactions and over 30 species [2]; the complete reaction mechanism of iso-octane oxidation includes 3600 elementary reactions among 860 chemical species [3].

Due to computational resource limitations to perform Direct Numerical Simulation (DNS), for moderate to high Reynolds values, Large-Eddy Simulation (LES) seems to be the best alternative. LES turns attractive since only the sub-grid scales and chemical reactions need to be modelled; the large scales are fully resolved. The LES equations are closed by modelling the stress tensor with an eddy viscosity. Therefore, the application of LES requires appropriate sub-grid scale models, fast computers and accurate and robust methods [4].

The present work develops a numerical method for the solution of mixing and reacting flows inside a combustor. Such diffusion flow is characterised by the Damköhler value and the internal structure of the flame depends on the time needed to consume the reactants [8]. The numerical method is based on the finite difference explicit Runge-Kutta five-stage scheme. Numerical tests are carried out for Damköhler 300, Zel'dovich 10, Heat Release 10 and Schmidt and Prandtl both equal to 0.9.

2 Governing equations and solution procedure

The model used is based on a two-dimensional set of governing equations. Although transience and turbulence are intrinsically three-dimensional, much insight is gained when analysing a bidimensional situation. Moreover, due to difficulties in establishing a complete chemical kinetics scheme and limitations of computer resources, a reduced reaction mechanism is usually adopted to describe the combustion process [5]. Therefore, the model assumes the finite rate Arrhenius kinetics hypothesis

$$v_f[F] + v_o[O] \Rightarrow v_p[P] + heat \tag{1}$$

and the fluid thermochemical state at any point is given by an scalar $C_k = (C_f, C_o, C_p)$. The reacting Navier-Stokes equations include the time evolution of density, velocity, energy and chemical species; Favre-averaging, or density weighted Favre filtered, simplify the governing equations. The Favre averaged equations are writen, in Cartesian non-dimensional tensor notation, as:

Mass

$$\frac{\partial \bar{\rho}}{\partial t} + \frac{\partial (\bar{\rho}\tilde{u}_j)}{\partial x_j} = 0 \tag{2}$$

Momentum

$$\frac{\partial (\bar{\rho}\tilde{u}_i)}{\partial t} + \frac{\partial (\bar{\rho}\tilde{u}_i\tilde{u}_j)}{\partial x_j} = -\frac{\partial \bar{p}}{\partial x_i} + \frac{\partial}{\partial x_j}\left(\frac{\bar{\mu}}{R_e}\tau_{ij}\right) + \frac{\partial \sigma_{ij}}{\partial x_j} \tag{3}$$

Energy

$$\frac{\partial (\bar{\rho}\tilde{T})}{\partial t} + \frac{\partial (\bar{\rho}\tilde{u}_i\tilde{T})}{\partial x_i} = \frac{\partial}{\partial x_i}\left(\frac{\bar{\mu}}{R_e P_r}\frac{\partial \tilde{T}}{\partial x_i}\right) + \frac{\partial \theta}{\partial x_i} + v_p H_e \bar{\dot{w}} \tag{4}$$

Chemical species

$$\frac{\partial (\bar{\rho}\tilde{C}_k)}{\partial t} + \frac{\partial (\bar{\rho}\tilde{u}_i\tilde{C}_k)}{\partial x_i} = \frac{\partial}{\partial x_i}\left(\frac{\bar{\mu}}{R_e S_c}\frac{\partial \tilde{C}_k}{\partial x_i}\right) + \frac{\partial Y_k}{\partial x_i} \mp v_k \bar{\dot{w}} \tag{5}$$

Pressure

$$\bar{p} = \bar{\rho} R \tilde{T} \tag{6}$$

where $\tilde{\tau}_{ij} = \tilde{S}_{ij} - \frac{2}{3}\frac{\partial \tilde{v}_k}{\partial x_k}\delta_{ij}$ is the resolved stress tensor, $\tilde{S}_{ij} = \frac{1}{2}\left(\frac{\partial \tilde{u}_i}{\partial x_j} + \frac{\partial \tilde{u}_j}{\partial x_i}\right)$ the mean strain rate, $\bar{\dot{w}} = D_a(\bar{\rho}\tilde{C}_f)(\bar{\rho}\tilde{C}_o)e^{\frac{-Z}{T}}$ the reaction rate and $\bar{\mu}$ the viscosity. D_a is the Damköhler, P_r the Prandtl, S_c the Schmidt, Z the Zel'dovich and H_e the heat release parameter. Observe that viscosity and density fluctuations are neglected; viscosity is temperature dependent and varies as $\frac{\bar{\mu}}{\mu_o} = \left(\frac{\tilde{T}}{T_o}\right)^{3/4}$. The $\mp$ refers to the reactant consumption and product formation, respectively, and R is the gas mixture constant. Contribution arising from radiation is assumed to be negligible in the energy equation; it is important for large flames which appears in furnaces, spreading of buildings and wildland fires [6].

The sub-grid terms are conveniently modelled as:

$$\sigma_{i,j} = \bar{\rho}(\tilde{u_i u_j} - \tilde{u}_i\tilde{u}_j) = \frac{\mu_T}{R_{eT}}\tilde{\tau}_{ij} \tag{7}$$

$$\theta = \bar{\rho}(\tilde{u_i T} - \tilde{u}_i\tilde{T}) = \frac{\mu_T}{R_{eT}P_{rT}}\frac{\partial \tilde{T}}{\partial x_i} \tag{8}$$

$$Y_k = \bar{\rho}(\tilde{u_i C_k} - \tilde{u}_i\tilde{C}_k) = \frac{\mu_T}{R_{eT}S_{cT}}\frac{\partial \tilde{C}_k}{\partial x_i} \tag{9}$$

where $\mu_T = \bar{\rho}C\Delta^2|\tilde{S}|$ is the eddy viscosity given by the Smagorinsky model, $C = 0.1$ and $\Delta = (\Delta x \Delta y)^{1/2}$ the sub-grid characteristic length scale. The main drawbacks of Smagorinsky model are the incorrect prediction of the limiting behaviour near walls in laminar flows and the inability to properly take into account the transfer of energy from the small to the large scales with a fixed model coefficient [2]. To overcome the first difficulty a Van Driest damping function is employed; therefore, the turbulent viscosity is writen as $\mu_T = \bar{\rho}C\Delta^2(1-e^{y^+/26})^2|\tilde{S}|$. In this way, the LES equations are closed by modelling the stress tensor with an eddy viscosity.

Integration in time is performed using a third order low storage Runge-Kutta time-stepping scheme; spatial derivatives are calculated using a fourth order finite difference central approximation [7]. Usually fourth order space approximation is sufficient for mixing and reacting flow situations; it is required for all domain, including the boundary conditions.

2.1 Boundary conditions

The proper implementation of boundary conditions is always important when solving a set of differential equations. Consider the combustor geometry as shown in Fig. 1: no slip conditions are employed for velocity at solid walls; outgoing conditions are given as non-reflecting open boundary conditions and the pressure comes from the Poisson equation. Therefore, the boundary conditions can be summarised as follows (see Fig. 1):

For the south $(i, 1)$ and the north (i, nj) boundaries, results

$\tilde{u} = \tilde{v} = \frac{\partial \tilde{T}}{\partial y} = \frac{\partial \bar{p}}{\partial y} = \frac{\partial(\bar{\rho}\tilde{C}_k)}{\partial y} = \frac{\partial \bar{\rho}}{\partial y} = 0$

where $\partial\tilde{T}/\partial y = 0$ corresponds, for a grid point $(i, 1)$, to
$\tilde{T}_{i,1} = \frac{1}{11}\left[18\tilde{T}_{i,2} - 9\tilde{T}_{i,3} + 2\tilde{T}_{i,4} - 6\Delta x\frac{\partial\tilde{T}}{\partial y}\right] + O(\Delta x)^4$,
for example, and nj is the biggest j line index counter in the y direction.

For the west boundary $(1, j)$
$\tilde{T} = 1; \quad \tilde{C}_f = 0; \tilde{C}_o = 1; \tilde{C}_p = 0;$
$\bar{\rho} = 1; \quad \frac{\partial\bar{p}}{\partial x} = 0$
$\tilde{u} = 0.2; \quad \tilde{v} = 0$

except at fuel injection place where $\tilde{C}_f = 1$, $\tilde{C}_o = 0$, $\bar{\rho} = 10$ and $\tilde{u}_{max} = 1$, parabolic.

For the east boundary (ni, j) the convective condition results in
$\frac{\partial\phi}{\partial t} + u_c\frac{\partial\phi}{\partial x} = 0$

with $\bar{p} = 1$, where $\phi = [\bar{\rho}\ \tilde{u}\ \tilde{v}\ \tilde{T}\ \tilde{C}_f\ \tilde{C}_o\ \tilde{C}_p]^T$ and u_c is the convective velocity; these derivatives are fourth order approximated.

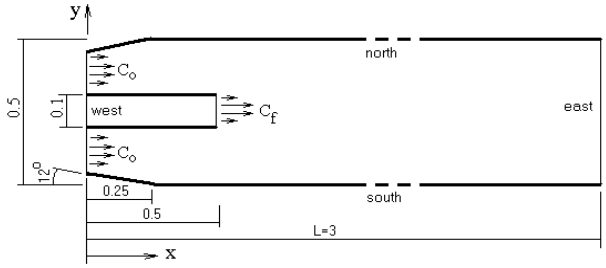

Fig. 1. Combustor geometry

3 Numerical results

Before solving the flow inside the combustor, numerical tests were realised solving the one-dimensional diffusion flame based on the laminar set of equations derived from (2-6); coherent results were obtained.

Following, the reacting flow inside the combustor, admitting that the fuel stream enters the aired environment with uniform velocity as indicated in Fig. 1, is analysed. The computational domain is rectangular and the grid contains 481x87 points. Body forces are used as in the immersed boundary method to enforce the boundary conditions and to define the geometry. It works well when the bonding surfaces are nearly flat or perpendicular to one another [4].

The time-step was chosen to be 5 x 10^{-6}, because the iterative process required to resolve the resulting system of equations has proven to be stiff [9]; observe that chemical source terms are exponential functions of the temperature.

Fig. 2 shows the velocity profiles at positions $x = L/4$, $x = L/2$ and $x = 3L/4$, respectively, for $D_a = 300$, $Z = 10$, $H_e = 10$ till 3.4 s. Recirculations surge at position $x = L/2$ while an expansion is observed at $x = 3L/4$; at position $x = L/4$ the velocity profiles indicate an accommodation of the mean jet during the 3.4 s; however, this configuration will probably disappear for longer times.

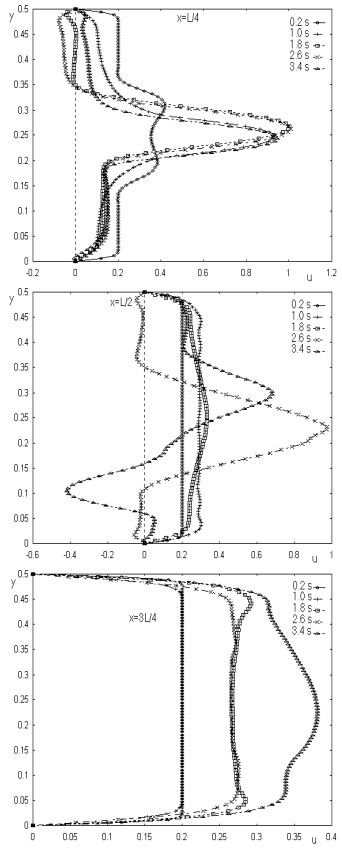

Fig. 2. Velocity profiles at positions x=L/4, L/2 and 3L/4, from 0.2 to 3.4 s

Fig. 3 indicates the product formation along the duct centerline. Such behaviour turns more clear when analysing the Fig. 4, which presents the vector map for the flow inside the combustor. Observe that the inflow and outflow boundary conditions do not introduce any significant spurious perturbation to the interior domain, as desired.

Diffusion waves are seen travelling to the direction of the walls; at solid walls they reflect increasing the flow complexity. The initial laminar jet distorts increasing the mixing and reaction rate inside the combustor; such occurs because

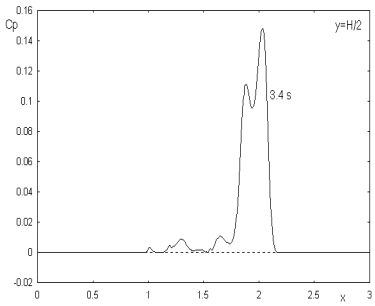

Fig. 3. Product along the duct centerline after 3.4 s

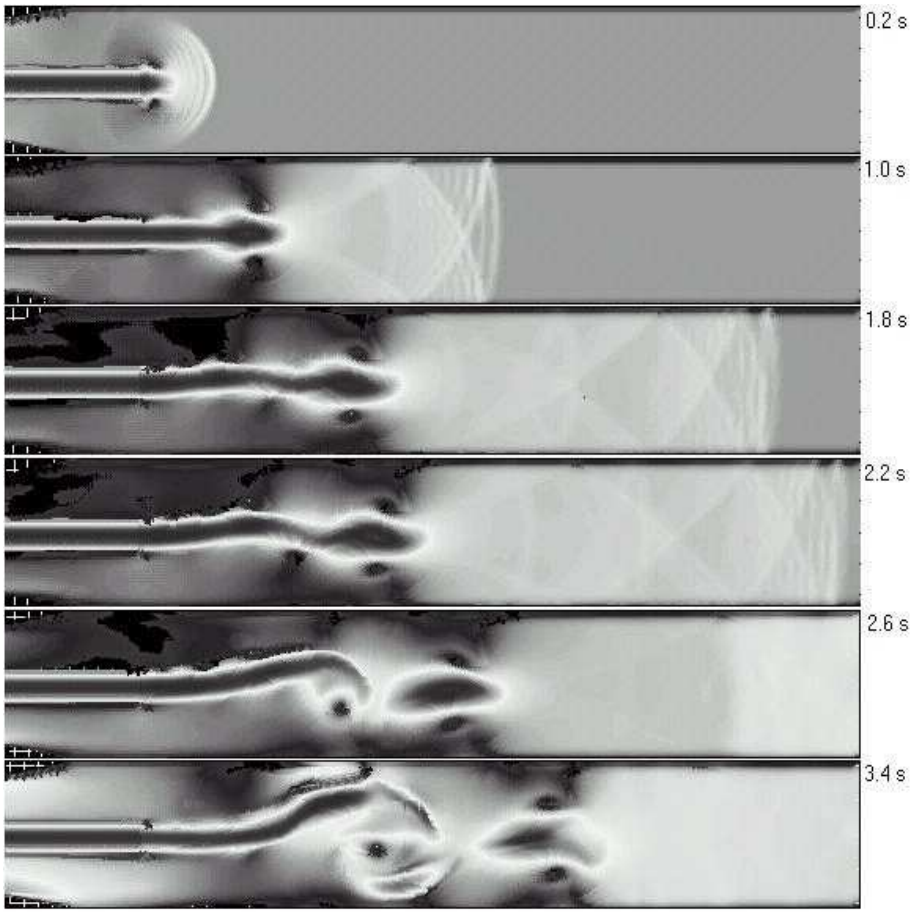

Fig. 4. Vector map inside the combustor till 3.4 s

of the vortices which are able to change the flow. It is clear that the asymmetry of the axial velocity profile, along the duct centerline, is a consequence of the diffusion which is by the flow expansion accelerated.

Remember that the structure of the diffusion flame depends on the time needed to consume the reactants [1], that means on the Damköhler value; when D_a is high ($D_a = 300$) the flow tends to the flamelet regime.

Fig. 5 left displays the temperature $\tilde{T}$ increase, the oxidiser $\tilde{C}_o$ consumption and the overall fuel $\tilde{C}_f$ increase inside the combustor; Fig. 5 right shows the product $\tilde{C}_p$ formation and the reaction rate RR till 3.4 s. Here, average means the mean value over all cells, that is for a variable ψ, $\psi_{average} = \frac{1}{ni.nj}\sum_{i,j}^{ni,nj}\psi_{i,j}$. Observe that after 2.4 s the temperature $\tilde{T}$, the product formation $\tilde{C}_p$ and the reaction rate increase considerably; such coincides with the wave front reaching the combustor exit.

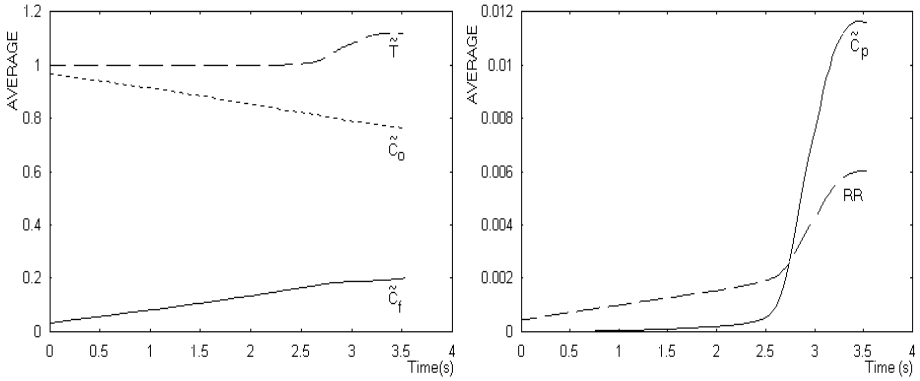

Fig. 5. Time evolution of temperature, oxidiser and fuel averages (left), of product and reaction rate averages (right) till 3.4 s

4 Conclusions

A LES computational model is developed which couples chemistry, fluid dynamics and heat transfer for solving the mixing and reacting flow inside a combustor. The numerical technique is based on the finite difference explicit Runge-Kutta five-stage scheme for third order time and fourth order space approximations, being fast, accurate, simple and cheap when using Cartesian co-ordinates.

Consistent results for product formation, temperature increase and reaction rate are obtained, showing that the model is able to follow non linear behaviour of the mixing and reacting progress for reasonable non-dimensional values for gaseous hydrocarbon chemistry.

The temperature gradient inside the flame cause the gas to expand rapidly and to form low density regions of small length scale [2]. The small scales tend to be isotropic in nature; they are less dependent on boundary conditions and flow type. Moreover, travelling waves are seen interacting with the walls; such turns the flow analysis more complex because it demands special care on the outflow boundary conditions.

For larger values of Reynolds the structure would present a continuous distortion, extension, production and dissipation of the flame surface by vortices of different scales [10]; such complex flow will be the objective of a future work.

5 Acknowledgements

The work reported in this paper has been supported by CNPq (*Conselho Nacional de Desenvolviomento Científico e Tecnológico - Brasil*) under process 310010/2003-9. Computations were performed on the computer Cray - T94 of CESUP-UFRGS. The support and assistance of the staff is gratefully acknowledged.

References

1. Vervisch, L., Poinsot, T.: Direct Numerical Simulation of Non-Premixed Turbulent Flames, Annu. Rev. Fluid Mech. **30** (1998) 655–691.
2. Liu, Y., Lau, K.S., Chan, C.K., Guo, Y.C. and Lin, W.Y.: Structures of Scalar Transport in 2D Transitional Jet Diffusion Flames by LES, Int. J. of Heat and Mass Transfer **46** (2003) 3841–3851.
3. Curran, H.J. Gaffuri, P., Pitz, W.J. and Westbrook, C.K.: A Comprehensive Modeling Study of Iso-Octane Oxidation, Combustion and Flame **129** (2002) 253–280.
4. Moin, P.: Advantages in Large Eddy Simulation Methodology for Complex Flows, Int. J. of Heat and Fluid Flow **23** (2002) 710–720.
5. Apte, S. and Yang, V.: Unsteady Flow Evolution and Combustion Dynamics of Homogeneous Solid Propellant in a Rocket Motor, Combustion and Flame **131** (2002) 110–131.
6. Law, C.K.: Heat and Mass Transfer in Combustion: Fundamental Concepts and Analytical Techniques, Prog. Energy Combust. Sci. **10** (1984) 295–318.
7. Anderson, D..A., Tannehill, J.C. and Pletcher, R.H.: Computational Fluid Mechanics and Heat Transfer, McGraw-Hill (1984).
8. Poinsot, T. and Veynante, D.: Theoretical and Numerical Combustion, R.T. Edwards Inc. (2005)
9. Baurle, R.A.: Modeling of High Speed Reacting Flow: Stablished Practices and Future Challenges, AIAA 2004-0267, Reno, Nevada (2004).
10. Renard, P.-H., Thévenin, D., Rolon, J.C. and Candel, S.: Dynamics of Flame/Vortex Interactions, Progress in Energy and Combustion Science **26** (2000) 225–282.